Structural topology optimization for multiple load cases using a dynamic aggregation technique

Kai A. James [a]; Jorn S. Hansen [a]; Joaquim R. R. A. Martins [a]
[a] Institute for Aerospace Studies, University of Toronto, Toronto, Ontario, Canada

PLEASE SCROLL DOWN FOR ARTICLE

Taylor & Francis
Taylor & Francis Group

Structural topology optimization for multiple load cases using a dynamic aggregation technique

Kai A. James*, Jorn S. Hansen and Joaquim R.R.A. Martins

Institute for Aerospace Studies, University of Toronto, 4925 Dufferin Street, Toronto, Ontario, M3H 5T6 Canada

A series of techniques is presented for overcoming some of the numerical instabilities associated with SIMP materials. These techniques are combined to create a robust topology optimization algorithm designed to be able to accommodate a large suite of problems that more closely resemble those found in industry applications. A variant of the Kreisselmeier–Steinhauser (KS) function in which the aggregation parameter is dynamically increased over the course of the optimization is used to handle multi-load problems. Results from this method are compared with those obtained using the bound formulation. It is shown that the KS aggregation method produces results superior to those of the bound formulation, which can be highly susceptible to local minima. Adaptive mesh-refinement is presented as a means of addressing the mesh-dependency problem. It is shown that successive mesh-refinement cycles can generate smooth, well-defined structures, and when used in combination with nine-node elements, virtually eliminate checkerboarding and flexural hinges.

Keywords: topology optimization; Kreisselmeier–Steinhauser function; adaptive mesh refinement; multiple load cases

1. Introduction

Since the its inception more than two decades ago (Bendsøe and Kikuchi 1988), topology optimization has undergone significant growth both in terms of its number of practitioners as well as the types of problems to which it is applied. Researchers from a wide range of disciplines and industries have adopted the method due to its ability to produce highly efficient, light-weight structures. A salient example of this trend is the Airbus A380 aircraft (Krog *et al.* 2004), in which topology optimization was used in the preliminary structural layout design of the leading edge and wingbox ribs. Examples such as this highlight the need for increased robustness in topology optimization algorithms. The desire to generate optimized topologies for feasible real-world structures demands that these frameworks come equipped with features and capabilities that take into account factors such as multiple load cases, material failure constraints, and buckling effects.

These considerations often give rise to optimization constraints that are difficult to implement due to numerical instabilities inherent in most topology optimization procedures. This article

---

*Corresponding author. Email: kai.james@utoronto.ca

presents several techniques for addressing these numerical instabilities with the goal of creating a robust framework that can be easily adapted to a wide-range of problems that involve multiple load cases and material failure constraints similar to those encountered in real-world applications. The techniques presented are designed to treat the problems of local minima, mesh-dependence, checkerboarding, and intermediate-density elements, all of which, if left untreated, can lead to drastically suboptimal and even unfeasible structures.

Because the standard topology optimization problem is highly non-convex, one must contend with the presence of up to thousands of local minima scattered throughout the design space. This means that optimal solutions are highly dependent upon the starting point and optimization search path followed. This phenomenon is especially apparent when handling multiple load cases. Previously used methods treat each load case as a separate constraint (Krog *et al.* 2004). However, the consequence of this approach is that those load cases, whose constraints are inactive at a given point in the search path, have minimal bearing on the subsequent search direction. This can lead to locally optimal solutions that perform poorly with respect to one or more load case. By performing constraint aggregation, one can mitigate this effect by ensuring that the optimizer retains sensitivity contributions from all load cases throughout the optimization. In this article, an adaptive version of the Kreisselmeier–Steinhauser function is used to aggregate either the objectives or constraints – in this case, maximum deflection – corresponding to each load case into a single function. The results are compared with those of established methods.

Additionally, a new technique for adaptive mesh refinement is presented. In typical topology optimization schemes, one must begin with a fine mesh in order to achieve high-resolution topologies. However, due to the mesh-dependency of the problem, this approach yields very thin members that may be difficult to manufacture and susceptible to failure by means other than those considered in the analysis such as buckling. Furthermore, it may require an excessive level of computational effort. While this problem can be eliminated with filtering techniques, these tend to produce fuzzy boundaries comprising regions of intermediate-density (Sigmund and Petersson 1998, Sigmund 2001). Adaptive mesh-refinement allows a designer to start with a relatively coarse mesh and then refine it only in locations where it is needed (Stainko 2006). This technique can produce members with realistic thickness and smooth surfaces with lower computational cost. The effectiveness of this method in reducing the occurrence of checkerboard patches and intermediate-density elements is also examined. This and other techniques described in this article have been tested on variations of the MBB beam problem, which is attributed to the the German aircraft company Messerschmitt–Bölkow–Blohm – MBB (Rozvany 1998).

2. Topology optimization with SIMP materials

Topology optimization is the process of determining the optimal number and configuration of structural members within a physical design domain in order to achieve a specific design objective. Typically, the domain is discretized into a uniform mesh of finite elements in which material will be either present or absent in the final solution. These individual elements combine to give a pixelized representation of the topology of the structure. The generalized topology optimization problem has the following form:

$$\min_{\mathbf{x}} : f(\mathbf{x}) \quad \mathbf{x} \in \mathbf{R}^n$$
$$\text{s.t.} : \mathbf{g}(\mathbf{x}) \leq 0$$
$$\mathbf{K}(\mathbf{x})\mathbf{u} - \mathbf{F} = 0$$
$$0 < x_{\min} \leq x_j \leq 1 \quad j = 1, \ldots, n.$$

Here f and $\mathbf{g}$ denote the objective and constraint functions, respectively, $\mathbf{F}$ and $\mathbf{u}$ are vector representations of the nodal applied forces and displacements, and $\mathbf{K}$ is the global stiffness matrix. The vector $\mathbf{x}$ represents the presence or absence ($x_j = 0$) of material within each element placed on the total weight or volume fraction of the optimized structure by including a constraint of the form

$$g = \frac{1}{n} \sum_{j=1}^{n} x_j - V_{\max} \leq 0, \tag{1}$$

where $V_{\max}$ is the fraction of the maximum allowable volume of the structure with respect to the total volume of the design domain. The resulting problem can be treated as a discrete one, in which case the design variables take on only the integer values 0 and 1. This problem can be solved using evolutionary algorithms (Jakiela *et al.* 2000). However due to the large number of design variables required to obtain a sufficiently well-defined design, the computational cost of these algorithms may be prohibitive and therefore they are seldom used.

Methods such as SIMP (Solid Isometric Material with Penalization) (Rozvany *et al.* 1992), and more recently, the level set method (Allaire *et al.* 2004), reframe the integer problem as a continuous one, allowing for the use of gradient-based optimization. Under the SIMP model element properties are assumed to be constant within an element and the *relative material density* is allowed to take on all real values between 0 and 1, with a density of zero indicating the absence of material. The effective material properties are given by

$$k_{\mathrm{e}} = x_{\mathrm{e}}^{p} k_0, \tag{2}$$

where $x_{\mathrm{e}} \in [x_{\min}, 1]$ represents the relative density of material within an element, k_0 is the value of the given material property, usually stiffness, in the solid phase (*i.e.* where $x_{\mathrm{e}} = 1$) and k_{e} is the effective value of the material property in the intermediate phase. With this formulation, an additional constraint of $x_{\mathrm{e}} > x_{\min}$, must be enforced to avoid singularities in the global stiffness matrix. The constant $x_{\min}$ must be a small number greater than machine zero and is typically chosen to be 0.001 so that elements with a density of $x = x_{\min}$ effectively mimic the behaviour of a void region. The parameter p is known as the penalization constant and is usually assigned a value such that $p \geq 3$ (Bendsøe and Sigmund 1999). This formulation makes the problem continuous while penalizing intermediate densities causing the solution to converge to a 0-1 design.

The use of SIMP penalization makes the problem highly non-convex (Sigmund and Petersson 1998) and so steps must be taken to reduce the likelihood of convergence to local minima. One approach is the *continuation method*, where the optimization begins with no penalization (*i.e.* $p = 1$) and the penalization constant is increased gradually over the course of the optimization until it reaches its terminal value (Sigmund and Petersson 1998). This will generally lead to lower objective values and superior designs. The method of moving asymptotes – MMA (Svanberg 1987) has been selected as the optimizer in this study, mostly due to its ability to accommodate the dynamically changing problems that result from continuation methods and other adaptive techniques. MMA is an interior point method that, during each major iteration, solves a convex subproblem based upon first-order sensitivity information at the current point in the design space. Because each subproblem is defined and solved independently of its predecessors, one can easily apply incremental changes to the problem parameters from one iteration to another.

In addition to local minima certain finite-element formulations can lead to *checkerboarding*, which is characterized by regions of alternating solid and void elements. The results presented use second-order finite elements, which virtually eliminate checkerboarding without producing the large grey regions associated with sensitivity filtering (Sigmund and Petersson 1998). Another problem related to finite element modelling is mesh dependence. The topology optimization problem as defined above is ill-posed and admits different solutions depending on the coarseness

of the finite-element mesh used. This problem, along with others, is addressed using the mesh-refinement technique described in Section 4.

3. Handling multiple load cases

When designing structures for complex systems such as aircraft, the handling of multiple load cases is an essential part of the design process, as a single aircraft may be subject to thousands of different loading conditions. When optimizing for minimum compliance, for example, many researchers simply include additional load cases by minimizing a weighted sum of the compliances under each load (Sigmund 2001, Krog *et al.* 2004, Pederson 2006). However, this method is inadequate if one wishes to optimize for the worst possible case, which often depends on the design itself. For this task one must use the bound formulation or an alternative form of min–max optimization.

3.1. *The bound formulation*

The bound formulation was introduced by Bendsøe *et al.* (1984) as a means of circumventing the lengthy process of generating a Pareto front and selecting the appropriate optimum. Although originally demonstrated on small, analytic problems (Bendsøe *et al.* 1984, Taylor and Bendsøe 1984), the method was subsequently extended to mathematical programming problems (Olhoff 1989). More recently, it has been used on large-scale topology optimization problems, as exemplified by Krog *et al.* (2004), who used this method for minimizing the compliance of wingbox ribs subject to multiple loading conditions. According to the method, one inserts a new objective β, which is to act as the upper bound on all other objectives, and treats the objectives from the original problem as constraints. Therefore, minimizing β is equivalent to minimizing the maximum of the original objective functions. The problem is formulated as follows:

$$\min_{\mathbf{x}} : \{\max\{f_i(\mathbf{x})\}\} \quad i = 1, 2, \ldots, m$$

$$\Updownarrow$$

$$\min_{\mathbf{x}, \beta} : \beta$$

$$\text{s.t.} : f_i - \beta \leq 0 \quad i = 1, 2, \ldots, m.$$

It should be noted that the variable β is appended to the vector of design variables $\mathbf{x}$, so that the new objective is simply a linear function of β.

3.2. *The Kreisselmeier–Steinhauser method*

The Kreisselmeier–Steinhauser (KS) function has been used by optimization researchers for a variety of multiobjective problems (Chattopadhyay and Seeley 1994), as well as problems involving local stress constraints (Striz 1994, Klimmek *et al.* 2002, Poon and Martins 2007). In the context of multiple load cases one seeks to minimize an aggregate objective function that is constructed using the values of the objectives corresponding to each individual load case as described by Equation (3) (Yang and Chahande 1995, Nishiwaki *et al.* 2001).

$$f_{\mathrm{KS}} = \frac{1}{\eta} \ln \sum_{i=1}^{m} \mathrm{e}^{\eta \bar{f}_i}, \tag{3}$$
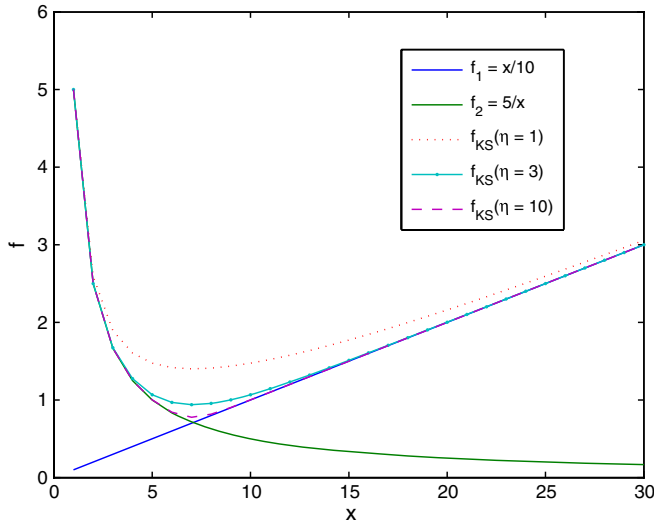
Figure 1. The KS aggregate of two arbitrary univariate functions using different values of the parameter η.

where

$$\bar{f}_i = \frac{f_i}{f_{0_{\max}}} - 1. \tag{4}$$

Here, the aggregate is modelled as an exponential envelope designed to closely resemble the non-smooth function $\max\{f_i\}$. All objective values are normalized with respect to the maximum initial objective value $f_{0_{\max}}$ so that $\bar{f}_i$ is on the order of 1. As shown in Figure 1, the aggregation parameter η dictates the closeness with which the KS function traces the function $\max\{f_i\}$. In the limit as η approaches infinity, $f_{KS} = \max\{f_i\}$. The parameter can be increased until an error of machine zero is achieved, however this makes the KS function non-smooth and causes unstable convergence. Poon and Martins (2007) proposed a solution that involved beginning with a nominal value of $\eta = 50$ and increasing it only as needed based upon the closeness of the design point to a constraint intersection. Shortly thereafter, París *et al.* (in press) applied the approach introduced by Poon and Martins to a topology optimization problem in which the local stresses in each element were aggregated using the KS function.

Extra care must be taken when choosing η for topology optimization problems, since in addition to the above-mentioned numerical challenges, one must also factor in the large number of local minima. For this reason, the values chosen are significantly lower than those used by Poon and Martins (2007). Additionally, because the final solution can be highly sensitive to the choice of η, the traditional form of the KS function is replaced with a *graduated* KS function. In this approach, the aggregation parameter is increased incrementally as the optimization progresses in order to produce an effect similar to that of the continuation method mentioned earlier. This differs from the approach employed by Poon and Martins (2007) in that the increase occurs unconditionally, whereas in their method, η was increased to a target value only if the sensitivity of the KS function with respect to η surpassed a certain tolerance.

4. Mesh refinement

Mesh refinement is a common strategy used in finite-element analysis of large, complex structures. The basic idea is to refine only those elements that are in areas of interest (*i.e.* areas of high stress in

the case of stress analysis) in order to achieve the required accuracy with minimal computational cost. This ability to concentrate on areas of interest is particularly useful in SIMP structures, where one must also solve the structural response in void regions. As De Sturler *et al.* (2008) have shown, the combination of a coarse mesh in void regions with a fine mesh in sold regions leads to accurate and computationally inexpensive solutions. However, in topology optimization, mesh refinement also serves several additional functions. One of the main purposes of this and other mesh-refinement techniques used in topology optimization (Stainko 2006) is to generate smooth material surfaces. Because the topology of the structure is unknown prior to optimization, most algorithms begin with a mesh of uniform density, in which all elements are of roughly equal size. This fixed-mesh approach, however, fails to address the inherent ill-posedness of the problem which causes the final solution to be highly dependent upon the mesh size used. A coarse mesh results in a jagged, poorly defined material interface (see Figure 2b), while a fine mesh results in a structure containing large numbers of excessively thin members, which reduce manufacturability and may be susceptible to buckling and other failure modes not considered in the optimization (see Figure 2c).

By performing adaptive mesh refinement, one can eliminate the jagged boundaries associated with a coarse mesh, while preventing the occurrence of overly thin members using fewer computations than would be required for a fine, uniform mesh. The refinement procedure presented in this article begins with the standard topology optimization problem using a uniform mesh comprising nine-node quadratic elements. The initial optimization begins with no penalization (*i.e.* $p = 1$) and the penalization factor is incrementally increased with each iteration until it reaches its final value of three in accordance with the convention. The optimization continues until convergence,
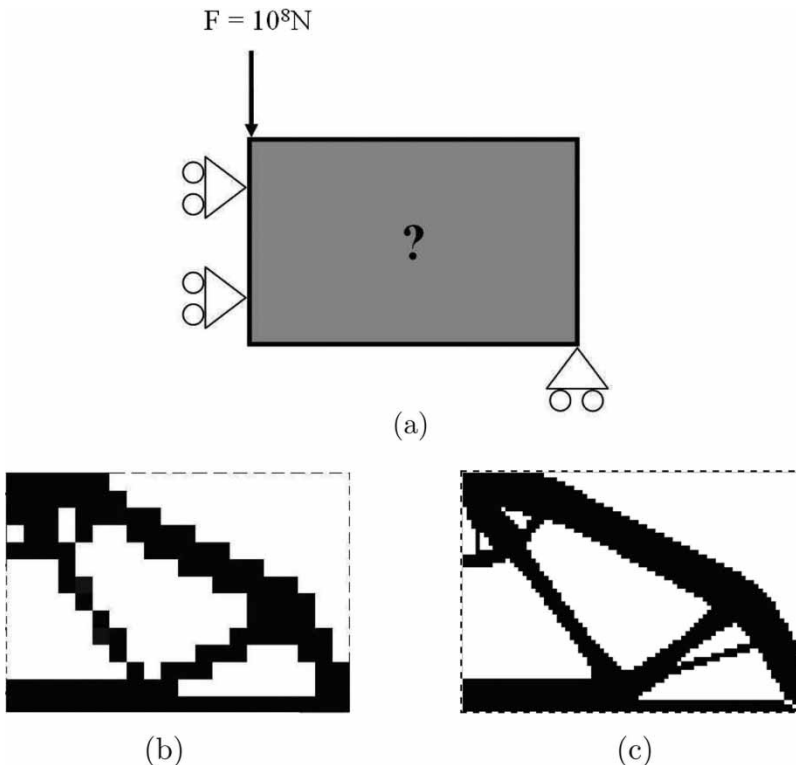

Figure 2.   Solutions to the half-MBB beam problem using both a coarse and a fine mesh.

with the convergence criterion defined as

$$\frac{|f(\mathbf{x}_k) - f(\mathbf{x}_{k-1})|}{|f(\mathbf{x}_k)|} < \varepsilon_{\text{conv}}, \tag{5}$$

where f is the objective function, $\mathbf{x}_k$ is the value of the design variable at the kth iteration, and $\varepsilon_{\text{conv}}$ is the convergence tolerance, which is set to 10^{-5}.

Upon convergence, all solid elements as well as void elements located along the solid–void interface are refined into four smaller square elements, whose side lengths are one half that of the original elements. Using this criterion, all elements that are adjacent, either orthogonally or diagonally to an element of the opposite state are flagged for refinement. Following this step, the optimization is performed again and this process is repeated until one reaches the desired degree of smoothness. During all stages following the initial refinement an additional restriction must be imposed to ensure that no two adjacent elements differ in size by more than one refinement level. This ensures that no element edge contains more than two hanging nodes.

Because local minima tend to occur at *binary* locations (*i.e.* all design variables have values 0 or 1), it is preferred that optimization searches start at *neutral* points (*i.e.* design points for which all design variables have intermediate values $x_i \approx 0.5$) within the design space. Therefore, although the unrefined solution is clearly suboptimal with respect to the refined problem, SIMP penalization may cause convergence to a local minimum within the vicinity of the binary, pre-refinement solution. This is true of any SIMP problem where a binary starting point is used, as this biases the final solution and renders the optimization search stagnant.

Removing the penalization altogether would result in a layer of intermediate-density elements scattered along the material interface as shown in Figure 3. This obscures the location of the true material interface making it difficult to perform the necessary post-processing of the design and also impeding further mesh-refinement. Instead, a strategy that exploits the duality of the weight-constrained topology optimization problem is relied upon here. The technique involves the penalization of material weight as opposed to the stiffness of intermediate densities as is traditionally done in the SIMP model. The penalization equation shown in Figure 4, has the following form:

$$\rho_i = x_i^{1/p}, \quad p > 1, \tag{6}$$

where ρ_i is the density of element i. Here, the penalization factor p is assigned a value of 2. This differs from most topology optimization schemes where the element density is assumed to be equal to the design variable x_i and, in fact, the two symbols are often used interchangeably to denote the same variable. Under this formulation, the effective element stiffness described in Equation (2) becomes $k_j = x_j k_0$, where the stiffness penalization has been removed and the design variable x_j is no longer the relative material density but rather a non-physical quantity whose value determines the material density via Equation (6).

The idea of penalizing weight is analogous to the original penalization method introduced by Zhou and Rozvany (1991). In their study they sought an equation that would effectively penalize
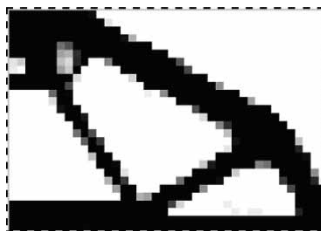
Figure 3.   Solution to the half MBB beam problem after one refinement with no penalization.
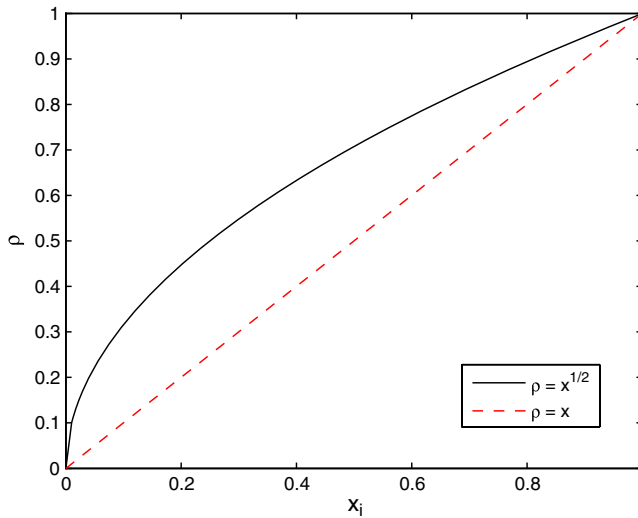
Figure 4.   The weight penalization function.

intermediate densities. The penalization function was interpreted as a cost function used to model the sum of the raw material and the manufacturing cost. The idea being that intermediate-density material, which is really solid material with an infinite number of tiny perforations, is much more costly to manufacture than its solid counterpart.

By increasing the perceived weight of intermediate-density material, especially that which is at the lower end of the density spectrum, one effectively lowers the acceptable material volume. This forces the removal of material from low priority areas in order to satisfy the volume constraint. The implicit reduction in the allowed volume fraction instantaneously reshapes the design space in order to overcome the binary stagnation problem. Alternatively, this effect can be interpreted as follows. With the addition of this new penalization factor, the stiffness penalization can safely be removed. The result is similar to that shown in Figure 3, with the only difference being that the penalization of low-density material effectively suppresses the prevalence of the outer layer of intermediate-density elements.

This procedure was tested on the half MBB beam problem described in Figure 2a, where compliance was minimized subject to a volume fraction constraint of 0.4. Beginning with the second refinement and continuing through later ones, the optimizer progressively adds material to the voids along the interface using the newly available smaller elements, eventually creating a smooth boundary.

Because material is removed after the first refinement, the first step in the process results in an increase in the objective value. However this increase is effectively negated as further refinements are performed. During the second phase of the refinement, the penalized volume fraction increases and approaches the actual prescribed volume fraction. Figure 6 shows the convergence history of the objective function. As shown in Figure 5, this method produces very smooth boundaries

Table 1.   Design parameters at various stages of refinement.

| Refinement stage	0	1	2	3
Number of iterations completed	100	125	150	175
Volume fraction	0.400	0.314	0.330	0.377
Compliance (J)	5.76×10^6	6.57×10^6	6.17×10^6	5.90×10^6
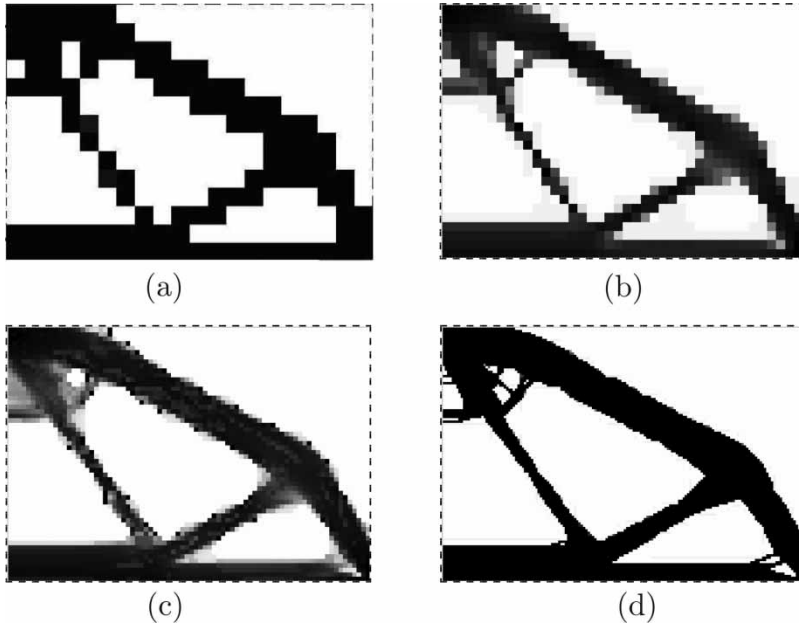
Figure 5. Results for mesh refinement using weight penalization; $\rho = x^{1/2}$.
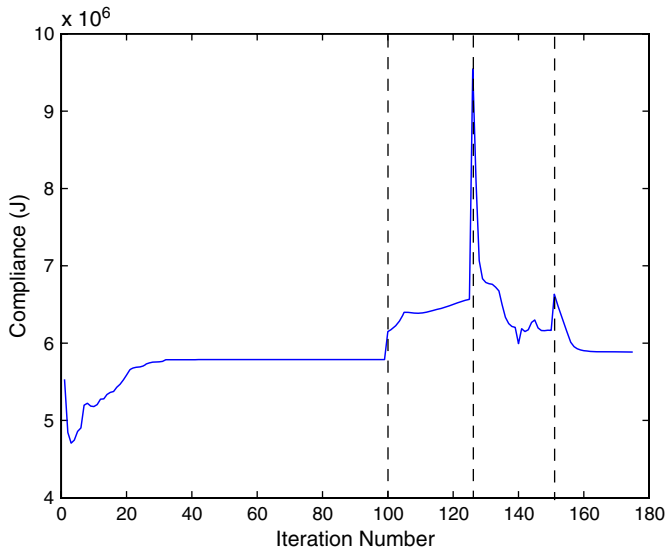
Figure 6. Convergence history for the mesh-refinement problem. Dashed lines indicate where refinement took place.

and can also reduce the occurrence of flexural hinges, which are a common problem encountered when not using filtering techniques.

5. Numerical results

The methods outlined above have been tested on the series of multiple-load MBB beam problems shown in Figure 7. Each point load constitutes a separate load case, and loads and supports are
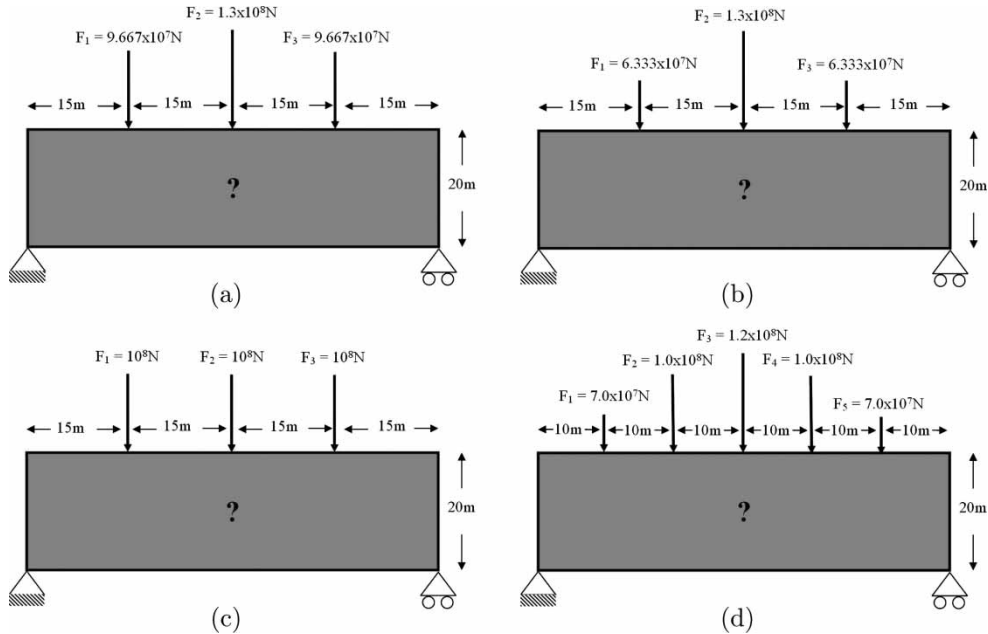
Figure 7. Geometry and loading configurations for test problems. Each problem contains 20×60 elements. $E = 10^{11}$ Pa; $\nu = 0.3$.

distributed across two elements to avoid strain concentrations. In the first group of problems, the maximum of the deflections under each load case was minimized and a volume constraint was enforced so that the total volume of the structure did not exceed 40% of the whole domain. The resulting problem formulation is shown in Equation (7):

$$
\begin{aligned}
&\min_{\mathbf{x}} : \quad \max_{i}\{\mathbf{L}_i\mathbf{u}(\mathbf{x})\} \quad \mathbf{x} \in \mathbf{R}^n \quad i = 1, \ldots, m \\
&\text{s.t.} : \quad \frac{1}{n}\left[\sum_{j=1}^{n}\rho_j(x_j)\right] - 0.4 \leq 0 \quad j = 1, \ldots, n \\
&\qquad \mathbf{K}(\mathbf{x})\mathbf{u} - \mathbf{F} = 0 \\
&\qquad 0 < x_{\min} \leq x_j \leq 1.
\end{aligned}
\tag{7}
$$

Here, the deflection under a given load i is defined as the mean of the vertical deflections of the nodes to which the force is applied. This mean is obtained via pre-multiplication of the nodal displacement vector $\mathbf{u}$ with the appropriate load-defining unit vector $\mathbf{L}_i$. In calculating the mean, the deflections of the two outer nodes for each load case have been assigned half the weighting given to the deflections at the inner nodes. This weighting corresponds to the nodal forces of the consistent force vector used in the finite element analysis, thus ensuring that the problem remains self-adjoint.

Additional experiments were performed in which the total volume was minimized subject to a constraint on the maximum deflection under each load. For these problems, the KS aggregate of the individual deflection constraints was provided to the optimizer as a single constraint. The results from this approach were then compared with those obtained by having the optimizer treat each constraint individually. This approach has been denoted using the abbreviation IC. All optimizations were performed using the method of moving asymptotes (MMA), with an imposed move limit of 0.2 on the design variables.

Problems were solved using varying values of the aggregation parameter η. In cases where the *graduated* KS function was used, the aggregation parameter was increased according to the following step function:

$$\eta = \begin{cases} 10 \leftarrow 1 \leq k \leq 30 \\ 30 \leftarrow 31 \leq k \leq 40 \\ 40 \leftarrow 41 \leq k \leq 50 \\ 50 \leftarrow 51 \leq k, \end{cases} \tag{8}$$

where the index k tracks the major iteration cycles.

5.1. *Deflection minimization*

Table 2 lists the deflection minimization results for Problem 1 using various values of the aggregation parameter η. Results indicate that setting η too high can lead to poor performance as the optimizer is provided with a minimal sensitivity contribution from the non-critical load cases, which results in convergence to local minima. Conversely, it is clear that if the parameter is set too low (*e.g.* $\eta = 1$), the KS function will offer a poor approximation to the min–max function, which also results in suboptimal designs. Among the instances when η is kept constant, the best result is obtained with a value of $\eta = 10$, which is a compromise between the two extremes. However, this result was improved upon slightly by increasing η over the course of the optimization search as shown in the Table 2.

Figure 8a shows the optimized design found when holding the aggregation parameter constant at $\eta = 50$. The high degree of asymmetry indicates that the solution is a local minimum and is, therefore, suboptimal. This characteristic is also present in the bound formulation solution (Figure 8b) although to a lesser extent.

Table 2. Maximum deflection (mm); load set 1.

| η	KS					BF
	1	10	30	50	10–50	
Load 1	21.7640	32.8366	30.6276	39.7368	33.6714	36.6412
Load 2	**36.9231**	**36.1451**	**37.3261**	**43.8992**	**35.9062**	**36.6451**
Load 3	21.7770	31.9858	32.1487	39.6114	32.8187	36.6415
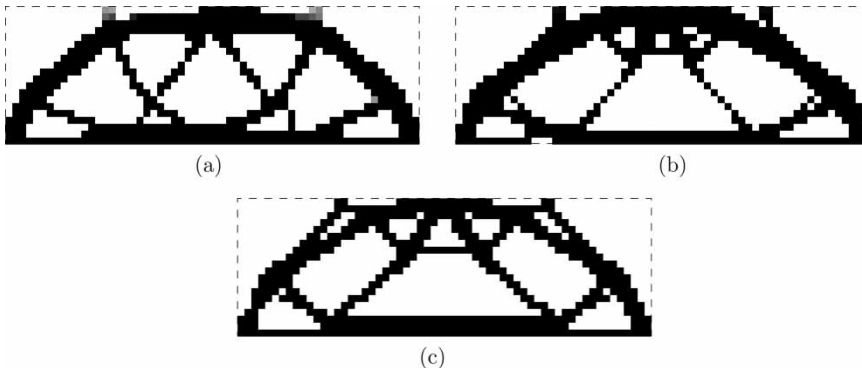
Figure 8. Optimized topologies for Problem 1.

The convergence plots for these solutions offer some insight into the source of the asymmetry. The bound formulation and the KS function with constant-η (Figures 9b and 9a, respectively) both produce oscillatory convergence histories, whereas the graduated-KS approach (Figure 9c) leads to a smooth convergence plot. These oscillations indicate that in the $\eta = 50$ case, the largest deflection dominates the objective function so that the optimizer progresses toward a design that performs well with respect to that particular load case. By the time this load case ceases to produce the largest deflection, the design has become irreversibly biased toward the current design, which causes the asymmetry and the poor objective values. This also occurs with the bound formulation. The bound formulation is further hampered by the fact that as the SIMP penalty parameter is increased from one iteration to another, this may cause a sudden breach of the objective-based constraints.[1] However, this effect is not sufficient to negate the benefits of the continuation method since using a constant penalty parameter yields even worse results.

In Problem 2, the magnitudes of the applied forces in the outer load cases are reduced, further increasing the disparity between critical and non-critical cases. The results in Table 3 show that, again, the graduated-KS function generates the best design, while the bound formulation converges to a solution whose maximum deflection is 10% higher that that of the graduated-KS design. It should be noted that, in Table 3, only the deflections produced by the *worst* load case from each problem are presented. Therefore each row corresponds to a different set of loading conditions.
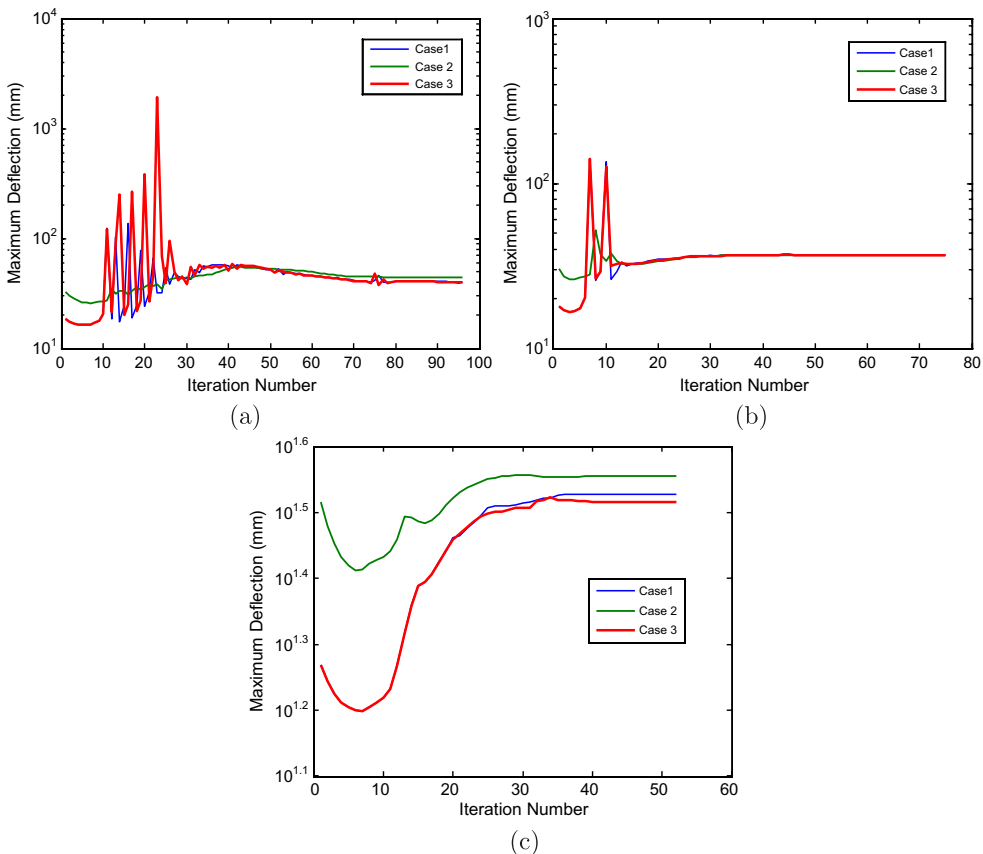

Figure 9.   Convergence histories for Problem 1.

Table 3. Worst case maximum deflection (mm); load sets 2 to 4.

	KS		
η	10	10–50	BF
Problem 2	33.7332	33.4366	36.8128
Problem 3	28.1604	28.0821	33.5804
Problem 4	24.8534	24.7688	25.7004

(a)   (b)
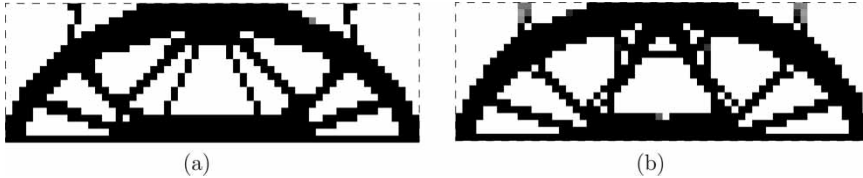
Figure 10. Optimized topologies for Problem 4.

The bound formulation was again compared with the graduated-KS approach and the constant-η KS method for Problem 3 in which all applied loads have equal magnitude. As shown in Table 3, the results for this problem are consistent with those obtained in Problems 1 and 2. In Problem 4, the number of load cases was increased to five and the prescribed volume fraction was increased to 50%. Figure 10 shows the optimized solutions for the bound formulation and graduated-KS approaches. In this case, the graduated-KS function outperforms the bound formulation by yielding a maximum deflection that is 4% smaller.

Table 4, along with Figure 11, shows what happens when the domain from Problem 1 is increased to 30×80 square elements with the domain dimensions increased accordingly. Here, the difference between the two approaches is more pronounced with the KS approach generating a maximum deflection nearly 11% smaller than that produced by the bound formulation. Again, the figures show that the two approaches produce visibly disparate results.

Table 4. Maximum deflection (mm); load set 1; 30×80 elements.

	KS	BF
Load 1	26.1798	20.6863
Load 2	**29.0994**	**32.6369**
Load 3	26.0914	21.4292

(a)   (b)
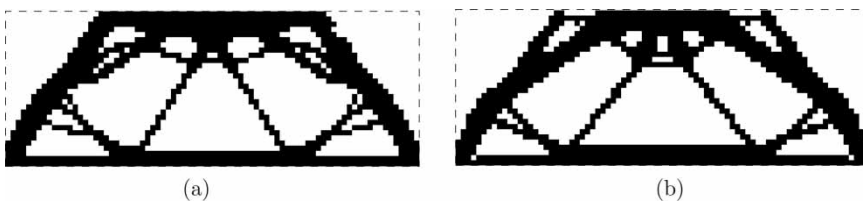
Figure 11. Optimized designs for Problem 1 using an increased domain size.

Downloaded By: [University of Michigan] At: 15:21 11 March 2010

Table 5. Weight minimization results for load set 1.

| | KS | | BF |
η	10	10–50	BF
Minimized volume (%)	48.3810	45.4979	46.7682
Maximum deflection (mm)			
Case 1	25.3302	28.5937	30.0080
Case 2	28.3344	29.8741	30.0035
Case 3	25.4254	28.5926	29.8966

Table 6. Weight minimization results for load set 2.

| | KS | | BF |
η	10	10–50	BF
Minimized volume (%)	46.1801	45.0258	63.0324
Maximum deflection (mm)			
Case 1	23.2748	27.9317	29.7216
Case 2	29.2924	29.9680	22.5424
Case 3	23.2055	27.9847	30.3397

5.2. *Weight minimization*

The observations outlined above also apply to the weight minimization problem. Using the load sets from Problems 1 and 2, with a prescribed maximum deflection of 30 mm, the KS method outperforms the method in which each constraint is handled individually (IC). Tables 5 and 6 show a breakdown of the results from load sets 1 and 2 respectively using both methods. It should be noted that the KS function used in this section is identical to that of the previous section with the only exception being that, in the minimum deflection problems, the deflection values are normalized with respect to the maximum initial deflection, whereas, in this section, the deflection values are normalized with respect to the maximum allowable deflection.

The numbers point to an increased disparity between the constant-η and graduated-KS approaches. This occurs because the KS function gives an overly conservative approximation to the min–max function at low values of η. Therefore, by increasing the parameter in a graduated fashion, one allows for a higher value of the maximum deflection thereby granting access to a larger portion of the feasible design space, while still preventing the oscillations associated with
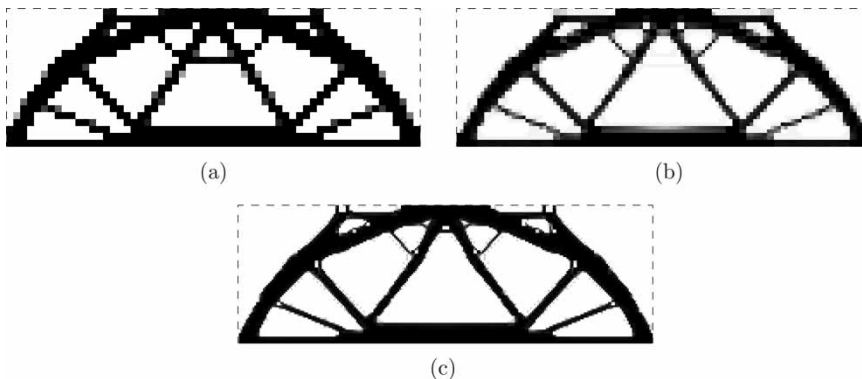

Figure 12. KS solution from Problem 1 using mesh-refinement.

high values of η. It should be noted that, unlike the deflection minimization problem, the SIMP penalization parameter p is kept constant throughout the optimization in order to ensure that the search path remains inside the feasible domain.

5.3. *Mesh refinement results*

The mesh-refinement technique was also used in combination with the KS function to produce smooth designs for problems involving multiple load cases. Figure 12 shows the results of applying the procedure to Problem 1 with a constant-η value of 10. As was the case in the single-load problem, flexural hinges along the thinner members and intermediate-density elements are virtually eliminated along with the jagged interfaces produced by the coarse mesh.

6. Conclusions

The results presented in this article show that the graduated Kreisselmeier–Steinhauser function can be used to generate robust structures when optimizing for multiple load cases. In numerical trials, this method consistently outperformed the bound formulation, which was prone to highly oscillatory convergence behaviour that resulted in inferior designs. It was also shown that local mesh refinement along the material interface could be used to produce well-defined, mesh independent designs and that by substituting the stiffness penalization for a weight penalization after the first refinement, one could overcome the problem of binary stagnation. When used in combination with nine-node elements, this technique offers a useful alternative to sensitivity filtering as it not only addresses the problem of mesh-dependency, but also reduces the occurrence of excessively thin member and flexural hinges.

   This result is significant since it shows that one can obtain feasible designs without creating intermediate-density elements, thereby opening the door for more sophisticated schemes that take into account material failure and buckling constraints. If researchers in industry can begin to incorporate these capabilities into the topology optimization design phase, they will ultimately produce lighter, more robust structures that may not be obtainable using the current sequential approaches. Further research should focus on developing accurate stress and buckling models for SIMP structures in order to take full advantage of these new methods.

Acknowledgements

Note

1. Although MMA is an interior point method, it performs a modification of the objective function that allows the search to extend beyond the limits of the feasible design space (Svanberg 1987).

References

Allaire, G., Jouve, F., and Toader, A., 2004. Structural optimization using sensitivity analysis and a level set method. *Journal of Computational Physics*, 194 (1), 363–393.
Bendsøe, M.P. and Kikuchi, N., 1988. Generating optimal topologies in structural design using a homogenization method. *Computational Methods in Applied Mechanics and Engineering*, 71 (2), 197–224.

Bendsøe, M.P., Olhoff, N., and Taylor, J.E., 1984. A variational formulation for multicriteria structural optimization. *Journal of Structural Mechanics*, 11 (4), 523–544.

Bendsøe, M.P. and Sigmund, O., 1999. Material interpolation schemes in topology optimization. *Archive of Applied Mechanics*, 69 (9–10), 635–654.

Chattopadhyay, A. and Seeley, C.E., 1994. A simulated annealing technique for multiobjective optimization of intelligent structures. *Smart Material Structures*, 3 (2), 98–108.

De Sturler, E., Paulino, G.H., and Wang S., 2008. Topology optimization with adaptive mesh refinement. *Proceedings of the 6th International Conference on Computation of Shell and Spatial Structures IASS-IACM 2008: 'Spanning Nano to Mega'*, Ithaca, New York, 28–31 May 2008.

Jakiela, M.J., *et al.*, 2000. Continuum structural topology design with genetic algorithms. *Computational Methods in Applied Mechanics and Engineering*, 186 (2–4), 339–356.

Klimmek, T., Kießling, F., and Hönlinger, H., 2002. Multidisciplinary wing optimization using a wingbox layout concept and a parametric thickness model. *In*: *9th AIAA/ISSMO Symposium on Multidisciplinary Analysis and Optimization*, Atlanta, GA, 4–6 September 2002, Paper AIAA-2002-5657.

Krog, L., *et al.*, 2004. Topology optimisation of aircraft wingbox ribs. *In*: *10th AIAA/ISSMO Multidisciplinary Analysis and Optimization Conference*, Albany, NY, 30 August–1 September 2004, Paper AIAA-2004-4481.

Nishiwaki, S., *et al.*, 2001. Optimal Structural design considering flexibility. *Computational Methods in Applied Mechanics and Engineering*, 190 (34), 4457–4504.

Olhoff, N., 1989. Multicriterion structural optimization via bound formulation and mathematical programming. *Journal of Structural Mechanics*, 1 (1), 11–17.

París, J., *et al.*, 2008 . Topology optimization of continuum structures with local and global stress constraints. *Structural and Multidisciplinary Optimization*. Available online at http://www.springerlink.com/content/c50p578416281541.

Pederson, P., 2006. Aspects of 3D shape and topology optimization with multiple load cases. *In*: *3rd European Conference on Computational Mechanics of Solids, Structures and Coupled Problems in Engineering*, Lisbon, Portugal, 5–8 June 2006.

Poon, N.M.K. and Martins, J.R.R.A., 2007. An adaptive approach to constraint aggregation using adjoint sensitivity analysis. *Structural and Multidisciplinary Optimization*, 1 (30), 61–73.

Rozvany, G.I.N., 1998. Exact analytical solutions for some popular benchmark problems in topology optimization. *Structural Optimization*, 15 (1), 42–48.

Rozvany, G.I.N., Zhou, M., and Birker, T., 1992. Generalized shape optimization without homogenization. *Structural Optimization*, 4 (3–4), 250–252.

Sigmund, O., 2001. A 99 line topology optimization code written in matlab. *Structural and Multidisciplinary Optimization*, 21 (2), 120–127.

Sigmund, O. and Petersson, J., 1998. Numerical instabilities in topology optimization: a survey on procedures dealing with checkerboards, mesh-dependencies and local minima. *Structural Optimization*, 16 (1), 68–75.

Stainko, R., 2006. An adaptive multilevel approach to the minimal compliance problem in topology optimization. *Communications on Numerical Methods in Engineering*, 22(2), 109–118.

Striz, A.G., 1994. A new look at the simultaneous analysis and design of structures. *In*: *NASA/ASEE Summer Faculty Fellowship Program*, December 1994.

Svanberg, K., 1987. The method of moving asymptotes – a new method for structural optimization. *International Journal of Numerical Methods in Engineering*, 24 (2), 359–373.

Taylor, J.E. and Bendsøe, M.P., 1984. An interpretation for min–max structural design problems including a method for relaxing constraints. *International Journal of Solids and Structures*, 20 (4), 301–314.

Yang, R.J. and Chahande, A.I., 1995. Automotive applications of topology optimization. *Structural and Multidisciplinary Optimization*, 9(3–4), 245–249.

Zhou, M. and Rozvany, G.I.N., 1991. The COC algorithm – Part II: Topological, geometry and generalized shape optimization. *Computational Methods in Applied Mechanics and Engineering*, 89 (1–3), 309–336.